RSC Advances

On the solid-state formation of BaTiO3 nanocrystals from mechanically activated BaCO3 and TiO2 powders: Innovative mechanochemical processing, mechanism involved, phase and nanostructure evolutions

Journal:	*RSC Advances*
Manuscript ID	RA-ART-11-2015-022942.R1
Article Type:	Paper
Date Submitted by the Author:	16-Dec-2015
Complete List of Authors:	Ashiri, Rouholah; Islamic Azad University, Materials Science
Subject area & keyword:	Nanomaterials - Materials < Materials

On the solid-state formation of $BaTiO_3$ nanocrystals from mechanically activated $BaCO_3$ and TiO_2 powders: Innovative mechanochemical processing, mechanism involved, phase and nanostructure evolutions

Rouholah Ashiri*

Department of Materials Science and Engineering, Dezful branch, Islamic Azad University, P.O. Box 313, Dezful, Iran

Abstract:

It still remains a challenge for the scientific community to obtain high quality barium titanate nanocrystals using high energy ball mills while avoiding unwanted (carbonate) by-products. The current work aims to address this challenge. In order to improve the kinetics of barium titanate formation, the starting materials, $BaCO_3$ and TiO_2, were mechanically activated with a high energy ball mill before their mixing and initiating the solid-state reaction. This step induces anatase to rutile polymorphic transformation simultaneous with particle refinement for TiO_2 starting particles while $BaCO_3$ do not experience any transformation during its refinement. Very fine monosized barium titanate nanocrystals free from the secondary phases and by-products are obtained at a lower calcination temperature. The progress of reactions for the formation of barium titanate is monitored by analyzing the X-ray diffraction patterns and DTA results. According to the proposed mechanism of formation, the formation of $BaTiO_3$ in the initial stage of the interfacial reaction between $BaCO_3$ and TiO_2 depends on the $BaCO_3$ decomposition. Mechanical activation of the $BaCO_3$ accelerates its decomposition and as a result barium titanate is obtained at a lower temperature and shorter time span in contrast to the literature. Moreover, the mechanical activation reduces the size of the starting materials and increases their specific surface area and stored energy. The high energy sites are potential sites for the nucleation of barium titanate crystallites during calcination and as a consequence a large density of fine crystallites is obtained. In the second stage, the barium titanate formation is controlled by Ba^{2+} diffusion through the formed barium titanate layer which acts as an inhibiting layer against further Ba^{2+} diffusion. The creation of a high density of lattice defects, dislocations and free surfaces during mechanical activation of the starting materials activates short-circuit diffusion paths and in turn accelerated the formation of pure single-phase barium titanate. In this stage, in contrast to the literature, no secondary phase and by-product was detected. The synthesis of barium titanate through this avenue is attractive for large-scale production and device application and may provide a strategy for the synthesis of other perovskites.

* Corresponding author Tel.: +98 9166447795; Fax: +98 6416260890
Email address: ro_ashiri@yahoo.com

Keywords: Solid-state reaction; Mechanical activation; High energy ball mill; Starting materials; Kinetics.

1. Introduction

Ferroelectric materials have a wide range of applications in electronic and electro-optic devices such as high-dielectric constant multilayer ceramic capacitors (MLCC), underwater transducers, pyroelectric sensors, medical diagnostic transducers, electro-optical light valves and electroluminescent panels [1-3]. Perovskite subgroup of the ferroelectric materials is the most important and thus the most widely studied one. Perovskite is usually expressed as ABO_3. Among the perovskite materials, barium titanate ($BaTiO_3$, BTO) is the best known and widely used ferroelectric material which has been intensively studied due to its excellent dielectric, ferroelectric and piezoelectric properties [4-8]. Moreover, BTO is regarded to be quite useful for the further development of the electronics industry especially for MLCCs [9-10]. To fabricate high capacitance small size MLCCs, BTO particles smaller than 100 nm with improved quality and uniform size are required. On the other hand, the characteristics of electronic ceramic powders are markedly influenced by their purity, particle size and morphology [11-13]. From these standpoints, production of BTO nanopowders with high purity, desired particle size and morphology has been gaining importance in recent times.

It is known that fine, homogeneous, and dispersive nanosized powders are necessary for the development of uniform microstructure and desired properties. Two major approaches are generally considered for synthesis of BTO nanoparticles [14]; traditional solid-state reaction using ball mills [4, 7, 9-10] and advanced processing routes such as sol–gel technique [14], hydrothermal synthesis [5] and sonochemical processing method [15]. However, the high-energy ball milling technique [16-18] is regarded as a simple and cost effective method for large scale

production of BTO powders from low cost starting precursors [11]. Traditionally, BTO powders are prepared through calcination of TiO_2 and $BaCO_3$ at high temperature of 1473-1573 K (1200-1300 °C) [4, 7, 9-10]. BTO powders prepared by this method usually have microscale average grain size, coarse uncontrolled and irregular morphologies, poor chemical homogeneity and less dispersion which are not suitable to realize very thin dielectric layers [14]. It still remains a challenge for the scientific community to obtain high quality BTO nanocrystals using high energy ball mills while avoiding unwanted by-products. Therefore, it is of more scientific and practical interests to study the possibility of producing very fine carbonate-free BTO nanocrystals by solid-phase reactions. On the other hand, to achieve the desired properties and practical applications, the quality of the BTO powders is very important, which depends strongly on their synthesis method [14]. Therefore, in order to obtain high quality BTO nanocrystals, it is important to select an appropriate milling method. In addition, although the calcination temperature has a significant role in controlling the microstructure of the final product, however the physical, chemical, or morphological properties of the starting powders also affect the final microstructure [13].

Basic challenging issues of powder preparation methods such as purity, homogeneity, size distribution and performance are encountered during solid-state preparation of BTO. Considering these facts and in view of above, we have tried to establish a new approach to obtain high quality BTO nanopowders. This work reports an innovative solid-state methodology to achieve BTO nanocrystals with controlled microstructural and morphological characteristics using mechanically activated $BaCO_3$ and TiO_2 as starting materials. The method also can be carried out at lower temperature in contrast to the literature [4, 7, 9-10] to obtain BTO nanopowders free of secondary phases. Moreover, the influence of the reactivity of the raw materials on the formation of BTO is studied. The synthesis of BTO through our established method may provide a

candidate for the large-scale synthesis of other perovskites. On the other hand, it is generally believed that [14] the physical properties of BTO nanoparticles are dependent upon their microstructure and morphology. Therefore, the phase evolution, microstructural and morphological characteristics of the obtained BTO powders are investigated, aiming at understanding the relationship between ball-milling conditions and the BTO powder characteristics.

2. Experimental procedure

In this work, BTO nanopowders were obtained from the solid-state reaction between $BaCO_3$ (Applichem; assay > 98 pct) and TiO_2 (Merck; assay > 99 pct) as the starting materials. Synthesis was performed in a planetary ball mill (Retch PM 400 in which the sun wheel and grinding jar rotate in opposite directions) under a highly pure argon atmosphere (99.999%) for various times. The planetary ball mill was set to a rotational mode that changes the rotational direction of the vial and the sun wheel every 6 min after a rest interval of 2 min. In all milling runs, the ball-to powder weight ratio was kept at 10:1 and the bowl rotation speed was 300 rpm. The hardened steel vial of 500 ml size and balls (10 mm diameter) were used. Moreover, all milling runs were performed at room temperature although a small increase in the temperature (about 20 K(°C)) of the bowl exterior was seen. To synthesize carbonate-free monosized BTO nanocrystals, the next steps were followed:

(i) in order to improve the kinetics of the synthesis reaction ($BaCO_3(s) + TiO_2(s) \rightarrow BaTiO_3(s) + CO_2(g)$), the starting materials, $BaCO_3$ and TiO_2, were mechanically activated using high energy milling for different times before their mixing. This innovative step was applied for the first time in this study. Our results presented in the

next section clearly show the contribution and effects of this step on the kinetics and mechanism of formation, microstructure and morphology of BTO powder products,

(ii) then, the mechanically activated $BaCO_3$ and TiO_2 were weighed in proportion to the stoichiometric ratio to yield $BaTiO_3$ (in 1:1 relation) and then homogeneously mixed with high energy ball mill at room temperature for 4 h,

(iii) the powder mixture then was thermally treated at 1173 K (900 °C) for 2h,

(iv) the obtained powders were washed with diluted formic acid in order to dissolve the (possible) remained carbonate by-products from the synthesized powder products.

The details of each step have been presented in the flowchart of the preparation method shown in Fig. 1

Crystalline phases and the structural analysis were carried out by an X-ray diffraction (XRD) technique. X-ray diffractometer (Philips PW3020) with monochromatic Cu Ka radiation (λ = 1.54178Å) was used over a 2θ angle from 20 to 70° to characterize the powders milled under different conditions and also to determine the crystallite size from the FWHM of the XRD peaks. The differential thermal analysis (DTA) measurements were performed using a thermal analysis system (STA 1500; Rheometric Scientific, Piscataway, NJ), in air, with a heating rate of 10 K(°C)/min, in a platinum crucible with α-Al_2O_3 powder as a reference. Because the samples might slowly react with crucibles, the cooling curves were not measured. The morphological features and microstructure of the products were observed by a field emission scanning electron microscope (FE-SEM; Hitachi S4160).

3. Results and discussion

It is known that multiple advantages of the solid-state method for obtaining BTO are that it is a single process and a cost-effective technique. Despite the advantages, there are some problems

which need to be solved. A high calcination temperature leads to coarsening of the BTO particles that are unsuitable for manufacturing fine grained ceramics and that, even the nominal ratio Ba/Ti in starting materials is 1, intermediate phases or $BaCO_3$ can persist as an end-product preventing the complete reaction between the starting materials. In this work, it had been tried to solve these drawbacks. The morphology and particle size of the unmilled starting materials (as-received precursors) are shown in Fig. 2. As can be seen in this figure, the needle-like particles are TiO_2 particles whereas the rounded ones are $BaCO_3$ particles. The microscale particles of TiO_2 have a larger size than $BaCO_3$ ones which are submicron sized.

In order to improve the kinetics of the reaction ($BaCO_3(s) + TiO_2(s) \rightarrow BaTiO_3(s) + CO_2(g)$) and also to solve the above mentioned drawbacks, the starting materials ($BaCO_3$ and TiO_2) were milled for different times before their mixing. There are some reports in the literature which have used a mechanical activation step just after mixing the starting materials [13], in those, the final BTO powder products (which have been calcined at much higher temperatures in contrast to the current work) contain some by-products and also non-reacted starting materials. Figs. 3 and 4 show XRD patterns and SEM micrographs of the TiO_2 and $BaCO_3$ starting powders as received and after different milling (mechanical activation) times. These XRD patterns indicate that in the first 10 h of the mechanical activation process, the broadening of TiO_2 and $BaCO_3$ peaks and a remarkable decrease in their intensities are observed as a result of refinement of the powders. Moreover, it can be said that the mechanical activation has induced a polymorphic transformation (anatase to rutile (see Fig. 3a)) in the TiO_2 powders while BCO powders has not experienced a phase transition and only particle refinement has occurred. This polymorphic transformation is directly related to the metastability of anatase. The size dependence of nanoparticles during a solid-state phase transformation has attracted much attention [19-20] because phase control is a key step to improve functionalities of the products for various applications. Metastability of

anatase and the severe conditions of the high energy ball mill used in this research rearrange the ordering and sequence of the TiO_6 octahedrals (see Fig. 5) existing in the anatase crystal structure resulting in the irreversible anatase-rutile phase transition. From the thermodynamic standpoint, rutile is more stable than anatase phase [21], but the formation of anatase especially in the wet chemical synthesis methods of TiO_2 is due to its rapid kinetic of formation. During the irreversible transitions, the atoms obtain freedom in motion from the metastable phase structure and then irreversibly transform into the most stable phase structure. Metastable states kinetically develop in the crystal growth reactions (especially during the wet chemical processing methods of preparation; in the case of the TiO_2 starting material used in this work due to its wet chemical synthesis) without reaching the stable state at each reaction step when the chemical bonds are too strong to free from the metastable states to the stable states. From this point of view, the phase of titanium dioxide depends on which of the phases grows faster during polymerization of TiO_6 octahedral units as the crystal nucleation. Severe mechanical activation by the high energy mills can activate this irreversible transformation. Some authors have reported that reaction conditions affect the phase and shape of TiO_2 nanoparticles obtained from crystal growth in the wet chemical processing methods due to the adsorption on reaction sites to inhabit growth of certain crystal structures or crystal faces [22-23]. As the first step of the crystal growth, tiny crystal nuclei for each crystal structure will form depending on its synthesis method and conditions. The difference in the crystal structure induced by the order of TiO_6 octahedral units; zigzag packing for anatase and linear packing for rutile (see Fig. 5). Although the linear packing results in the thermal stable structure due to the closest packing of TiO_6 octahedral units, the bridging structure is unstable under the kinetic control condition. Once the metastable anatase phase forms, it cannot transform to rutile without melting-like process because Ti-O bonds have strong binding energy as an ionic covalent bond [21]. But in the severe mechanical activation using high energy

mills, the impact-type compressive forces tend to rearrange the TiO_6 octahedral units to a closer packing state and as a result, the irreversible anatase to rutile polymorphic transformation occurs. Moreover, as can be seen in Fig. 4, the needle shape of the TiO_2 particles disappeared completely after 10 h milling time and the powders are agglomerated. It was found that the mechanical activation of the starting materials influences not only particle size and morphology but also development of the solid-state polymorphic transformation of TiO_2. It is not easy to mix the starting materials and maintain chemical homogeneity in the final product without the mechanical activation. As is evident in Figs. 3 and 4, the continuation of the mechanical activation up to 30 h leads to an increase in the powders refinement and also results in the progress toward the amorphization of structure of the starting materials. This is evident where the sharp crystalline diffraction peaks broadened and their intensities decreased progressively during mechanical activation process. For these samples, the halo pattern becomes more obvious due to existence of a large amount of amorphous phase in the milled powders and crystallite refinement. Moreover, as can be seen in Fig. 3, the fraction of the amorphous phase increased with milling time increasing, although the rate of amorphization gradually slowed down as mechanical activation proceeded. In this stage, the crystalline diffraction peaks did not shift very large during mechanical activation even at the very long times. Although, the particle refinement is main obvious outcome of this high energy milling (mechanical activation) step, however this step has several other more important effects which the method established here smartly uses them to obtain a better final BTO product. The following important effects are induced by this step:

(i) The particle refinement obtained after this step (see Fig. 4) increases the specific surface area and thus the reactivity of the precursors, which facilitates the formation of the final BTO product when mixing the precursors.

(ii) The finer particle size of the precursors can also guarantee the more homogenous mixing of the precursors during the successive step of preparation (see Fig. 1). This effect can prevent or reduce the formation of by-products in the final product such as secondary phases, non-reacted precursors and non-stoichiometric products. Formation of the unwanted secondary phases is the main drawback of the previously established solid-state processes [9-10, 13, 24].

(iii) The energy absorbed by the precursors in this step provides a lot of the suitable sites for nucleation of the final product during the calcination step. This can result in the formation of very fine monosized nanocrystals of BTO at the end of the synthesis pathway which normally cannot be obtained by the solid-state synthesis methods using the mechanical milling process.

(iv) The high specific surface area, high energy absorbed by the precursors, formation of a high density of crystal defects induced by mechanical activation stage effectively enhance the diffusion rate by activating the high diffusivity paths during calcination stage. This results in the formation of the final product at lower calcination temperature and shorter calcination time.

The next results will demonstrate these effects. Previous researches have used the mechanical activation after mixing the precursors [13, 24]. This mechanical activation does not have all of the above advantages and their final products have some problems with basic challenging issues of powder preparation methods such as purity, homogeneity, size distribution and performance.

Fig. 6 shows the XRD patterns of the starting and activated powders, and also after 4 h mixing by the high energy mill. Although 4 h milling for homogenous mixing the BCO and TiO_2 results in the particle refinement (disappearance of some peaks), but the most important peaks of the

starting powders did not disappeared in the XRD pattern of the mixture of the starting powders . For the activated BCO and TiO_2 powders, most of the characteristic peaks of the TiO_2 disappeared after mixing while the characteristic peaks of BCO persist toward disappearing. This indicates that the particle size of this material cannot be reduced more. Some shifts in the position of the peaks are seen in the mixture of the activated powders due to their more stored energy. Some traces of final product, BTO, are seen in the mixture of powders activated for 30 h which, suggest that critical activation time and thus particle refinement are required for the solid-state formation of BTO without any calcination process. This also indicates that with aid of these critical conditions, the decomposition of barium carbonate to barium oxide and carbon dioxide is possible. SEM micrographs presented in Fig. 7 indicate that mixing process increases the tendency of the agglomeration of the powders which can be attributed to the thermodynamics of mixing the BCO and TiO_2 which have mutual solubility.

DTA analysis was carried out in order to analyze the contribution of mechanical activation of the $BaCO_3$ and TiO_2 starting materials before their mixing on the formation of BTO. DTA curves (see Fig. 8) for different mixtures clearly showed the effect of the mechanical activation of the precursors. It is evident that the location of the peak appeared in the DTA curves depends on the pre-milling conditions of the TiO_2 and BCO starting powders. The reaction rate of the finer BCO and TiO_2 in mechanically activated sample is considerably higher than that of the non-activated one. For the coarser powder (sample (b) in Fig. 8), the mentioned peak is shifted to a higher temperature indicating the kinetics of formation of BTO in this sample is slower. Meanwhile, this suggests the possibility to attain complete conversion of precursors to BTO in a reasonable time even at a lower temperature using the mechanically activated TiO_2 and BCO powders.

XRD results (Fig. 9) indicate that the method used in this work leads to formation of the carbonate-free BTO nanoscale crystals with perovskite symmetry only by 2 h calcination at 1173 K(900 °C). BTO nanocrystals are characterized by well-resolved peaks at around 22.16, 31.56, 38.96, 45.24, 50.96, 56.24 and 65.88° corresponding to the (1 0 0), (1 1 0), (1 1 1), (2 0 0), (2 1 0), (2 1 1) and (2 2 0) planes, respectively. All peaks of the XRD patterns match well with standard cubic BTO perovskite phase JCPDS No. 31-174 confirming the formation of BTO with perovskite symmetry. The XRD patterns of the synthesized products are consistent with other reports [25-31]. The non-activated sample (without application of the milling step on the starting materials ($BaCO_3$ and TiO_2)) exhibits more intense peaks than mechanically activated one indicating its crystallites have grown more in contrast to those of mechanically activated sample. Considering the prominent (1 1 0) peak located at 31.56° and using the Scherrer formula given in Ref. [14], we estimate the average crystallite size of 10 h mechanically activated sample and non-activated sample to be 26.66 and 45.44 nm, respectively. These results indicate that our approach has led to a significant reduction in the size of the synthesized BTO crystallites. On the other hand, the peaks of carbonate phases are not observed in the pattern of this sample, therefore, it can be said that the final BTO product is carbonate-free. The above results indicate that very fine BTO nanocrystals free from any by-product have been obtained through the present synthesis pathway. As can be seen in Fig. 9, the location of XRD peaks in the pattern of the 10 h mechanically activated sample have shifted about 0.2° to lower 2θ in contrast to those of non-activated sample due to stored energy in the material during the mechanical activation stage of the starting powders. Moreover, as can be seen in this figure, the long time mechanical activation stage should be avoided due to formation of some by products (see the traces of the by-products at around 2Θ of 24 and 29° in the sample which was mechanically activated for 30 h). Meanwhile, the long time mechanical activation increases the costs of preparation.

Fig. 10 shows FE-SEM micrographs at different magnifications of BTO powder products synthesized in this work. As can be seen in this figure, the powders appear to be agglomerated caused primarily by the processes occurring during milling and calcination of the powder mixtures. Moreover, the small particles embedded in each agglomerated cluster correspond to the BTO nanocrystals. FE-SEM micrographs exhibit crystal size consistent with the average crystallite size determined by the analysis of XRD. The morphological properties and size distribution characterization of the mechanically activated sample indicate that the products consist of somewhat regularly shaped and relatively spherical particles with a narrow size distribution. Moreover, the SEM micrographs of mechanically activated (10 h) sample exhibit a larger density of finer crystallites in contrast to non-activated sample. The above results indicated that with the help of our approach, carbonate-free BTO particles with tailored morphology have been synthesized. Moreover, mechanical activation of the starting materials accelerates the homogeneous formation of BTO nanocrystals and can also be beneficial in controlling the size and shape of the nanocrystals. It is apparent from the FE-SEM micrographs that BTO nanocrystals observed in the agglomerates of mechanically activated sample are relatively uniform in size having spherical morphology than non-activated sample. There are some other papers describing synthesis of BTO by solid-state synthesis method without mechanically activation of the $BaCO_3$ and TiO_2 before their mixing; those methods produced poorly uniform and larger particles with board particles size distributions [10-11, 28-29, 32-34] at higher temperatures. However, the results indicate that we can obtain monosized particles with spherical morphology at lower temperatures in contrast to the literature [10-11, 28-29, 32-34]. Moreover, the lower calcination temperature results in weakly agglomerated powders and intensive milling is not required.

In this section, we discuss the role of the mechanical activation step of the $BaCO_3$ and TiO_2 starting powders on the formation of BTO nanocrystals. The mechanical activation step results in extensive formation of lattice defects, dislocations in particular, because of its induced severe plastic deformation. Moreover, this step reduces the size of the starting materials and thus increases their specific surface area and stored energy. A characteristic feature of all solid-state reactions is that they involve the formation of product phase at the interfaces of the starting materials. Then, growth of the product phase involves diffusion of atoms of the reactants through the product phase, which constitutes a barrier layer preventing further reaction. The solid-state reactions initiated by intensive milling in high-energy ball mills could be good choice for BTO powder preparation. An important criterion for intensive milling is the formation of highly dispersed phase materials for oxide based materials or the formation of new product because of a solid-state reaction. Intensive milling (mechanical activation) the starting materials increases the area of contact between the reactant powder particles due to reduction in particle size and allows fresh surfaces to come into contact. This effect results in homogenous mixing the starting materials, which prevents the formation of the secondary phases during the calcination treatment and as a result, BTO powder product free from secondary phases is obtained. EDAX analysis results also approve the role of the mechanical activation on the purity of the final BTO products. As can be seen in Fig. 11, the sample which was prepared without mechanical activation stage contains a large amount of carbon and thus carbonate by-products indicating this sample is not carbonate-free. It seems that the severe mechanical activation of barium carbonate activates the decomposition of barium carbonate to barium oxide and carbon dioxide. This is another effect of the mechanical activation stage. According to the reaction mechanism [14], the formation of BTO in the initial stage of the interfacial reaction between BCO and TiO_2 depends on the BCO decomposition. Mechanical activation helps this decomposition and in turn formation of BTO.

The milling stage of the starting materials is also characterized by intensive plastic deformation of the powder at extremely high strain rate, creation of a high density of defects. These sites (due to the stored energy in the starting materials during the milling process) are potential sites for the nucleation of BTO crystallites. This effect results in the formation of a large density of finer crystallites in the mechanically activated samples in contrast to the non-activated sample as is evident in SEM micrographs of Fig. 10. On the other hand, it has been demonstrated [14] that in the second stage, $BaTiO_3$ formation is controlled by barium diffusion through the formed barium titanate layer [35]. In this stage, in contrast to the literature, no secondary phase was detected [10-11, 28, 34]. The mechanical activation stage of the starting materials can effectively facilitate the diffusion process by providing high diffusivity paths through the creation of a high density of lattice defects, dislocations and free surfaces. These defects in turn accelerate the diffusion of Ba^{2+}.As a consequence, solid-state reactions that normally require high temperatures will occur at lower temperatures. In other words, the high density of defects induced by intensive milling of the starting materials favors the diffusion process required for BTO formation [36]. Meanwhile, the particle refinement and thus reduction in diffusion distances (due to microstructural refinement) reduces the reaction temperature and time significantly. Based on the above discussion, it can be said that mechanical activation reduced the formation temperature and accelerated the formation rate of BTO. Our observations indicate that BTO phase formation was greatly enhanced due to the refinement of the oxide precursors as a result of the high-energy milling (mechanical activation of the starting BCO powder). Moreover, critical parameters in the preparation of barium titanate nanopowders by solid-state reactions are the particle size of raw materials, the absence of large hard agglomerates, and the homogeneity of the mixture. The use of the mechanically activated raw materials improves these parameters and favors the formation of very fine BTO nanocrystals with a narrow size distribution at a lower calcination temperature

[37-39]. The conventional solid state processes [28-29, 10-11, 32-34] did not produce single phase nanosized BT at the same temperature and heating rate which were used in our work; the decomposition of BCO was incomplete. This indicates that mechanical activation step accelerated the formation kinetics of BTO from BCO and TiO_2. Our previous experiences in fabrication the nanoscale materials [14, 27, 35-36, 40-58] critically indicate that a smart designing of the process and the use of the properly selected starting materials (or precursors) significantly influence the microstructure and performance of the final nanoscale product.

Finally, it can be said that the method developed in this work can reduce particle size and enable obtaining the nanostructured BTO powders by solid-state process, which are of the main interest in current trend of miniaturization and integration of electronic components. Meanwhile, solid-state reaction of mechanically activated BCO and TiO_2 turns out to be an attractive process to obtain homogeneous nanopowders of BTO and a realistic alternative to more expensive wet-chemical routes. Moreover, this simple innovative method will offer a new strategy for preparing the nanoscale powders of other perovskite materials.

4. Concluding remarks

The present study described a simple low temperature method for obtaining very fine single-phase BTO nanopowders by an innovative solid-state reaction when mechanically activated $BaCO_3$ and TiO_2 were used as raw materials. The obtained nanopowders was characterized by X-ray diffraction (XRD), scanning electron microscopy (SEM), energy-dispersive X-ray spectroscopy (EDAX) and differential thermal analysis (DTA) techniques aided by theoretical calculations. The results give evidence of the strong effect of the mechanical activation on the solid-state formation of barium titanate. Mechanical activation reduced the formation temperature and accelerated the formation rate of BTO. BTO formation was favored by the catalytic effect of

very reactive TiO_2 and $BaCO_3$ due to their higher stored energy and higher specific surface area induced by mechanical activation stage. The mechanical activation also influenced particle size and morphology of the obtained BTO powders. We believe that the BTO nanoparticles prepared by the current approach can be used as the starting materials for the miniaturization of advanced MLCCs.

References

[1] M. T. Buscaglia, M. Bassoli, V. Buscaglia, Solid-State Synthesis of Nanocrystalline $BaTiO_3$: Reaction Kinetics and Powder Properties, J. Am. Ceram. Soc. 91 (2008) 2862–2869.

[2] L.B. Kong, T.S. Zhang, J. Ma, F. Boey, Progress in synthesis of ferroelectric ceramic materials via high-energy mechanochemical technique, Prog. Mater. Sci. 53 (2008) 207–322.

[3] X. He, J. Ouyang, J. Jin, H. Yang, Rapid synthesis of barium titanate microcubes using composite-hydroxides-mediated avenue, Mater. Res. Bull. 52 (2014) 108–111.

[4] Ch. Chang, Ch. Huang, Y. Wua, Ch. Sub, Ch. Huang, Synthesis of submicron $BaTiO_3$ particles by modified solid-state reaction method, J. Allo. Compd. 495 (2010) 108–112.

[5] X. Zhu, J. Zhu, Sh. Zhou, Zh. Liu, N. Ming, Hydrothermal synthesis of nanocrystalline $BaTiO_3$ particles and structural characterization by high-resolution transmission electron microscopy, J. Cryst. Grow. 310 (2008) 434–441.

[6] V. Buscaglia, M. Viviani, M.T. Buscaglia, P. Nanni, L. Mitoseriu, A. Testino, E. Stytsenko, M. Daglish, Z. Zhao, M. Nygren, Nanostructured barium titanate ceramics, Powder Technol. 148 (2004) 24–27.

[7] E. Brzozowski, M.S. Castro, Synthesis of barium titanate improved by modifications in the kinetics of the solid state reaction, J. Euro. Ceram. Soc. 20 (2000) 2347–2351.

[8] S. Kwon, K. Choi, B. Kim, Solvothermal synthesis of nano-sized tetragonal barium titanate powders, Mater. Lett. 60 (2006) 979–982.

[9] A.K. Nath, C. Jiten, K.C. Singh, Influence of ball milling parameters on the particle size of barium titanate nanocrystalline powders, Phys. B405 (2010) 430–434.

[10] M. T. Buscaglia, M. Bassoli, V. Buscaglia, Solid-State Synthesis of Ultrafine $BaTiO_3$ Powders from Nanocrystalline $BaCO_3$ and TiO_2, J. Am. Ceram. Soc. 88 (2005) 2374–2379.

[11] A.C. Roy, D. Mohanta, Structural and ferroelectric properties of solid-state derived carbonate-free barium titanate ($BaTiO_3$) nanoscale particles, Scripta Mater. 61 (2009) 891–894.

[12] W. Chaisan, R. Yimnirun, S. Ananta, Effect of vibro-milling time on phase formation and particlesize of barium titanate nanopowders, Ceram. Int. 35 (2009) 173–176.

[13] C. Gomez-Yanez, C. Benitez, H. Balmori-Ramirez, Mechanical activation of the synthesis reaction of $BaTiO_3$ from a mixture of $BaCO_3$ and TiO_2 powders, Ceram. Int. 26 (2000) 271–277.

[14] R. Ashiri, Analysis and Characterization of Phase Evolution of Nanosized $BaTiO_3$ Powder Synthesized Through a Chemically Modified Sol-Gel Process, Metall. Mat. Trans. A 43 (2012) 4414-4426.

[15] K. Yasui, T. Tuziuti, K. Kato, Numerical simulations of sonochemical production of $BaTiO_3$ nanoparticles, Ultrason. Sonochem. 18 (2011) 1211–1217.

[16] C. Suryanarayana, Mechanical alloying and milling, Prog. Mater. Sci. 46 (2001) 1–184.

[17] D. L. Zhang, Processing of advanced materials using high-energy mechanical milling, Prog. Mater. Sci. 49 (2004) 537–560.

[18] C. Suryanarayana, E. Ivanov, V.V. Boldyrev, The science and technology of mechanical alloying, Mater. Sci. Eng. A304–306 (2001) 151–158.

[19] S. H. Tolbert, A. P. Alivisatos, Size dependence of a first order solid-solid phase transition: the wurtzite to rock salt transformation in CdSe nanocrystals, Science 265 (1994) 373–376.

[20] K. Jacobs, D. Zaziski, E. C. Scher, A. B. Herhold, A. P. Alivisatos, Activation volumes for solid-solid transformations in nanocrystals, Science 293 (2001)1803–1806.

[21] N. Satoh, T. Nakashima, K. Yamamoto, Metastability of anatase: size dependent and irreversible anatase-rutile phase transition in atomic-level precise titania, Sci. Rep. 3 (2013) 1–6.

[22] Y.-W. Jun, Surfactant-assisted elimination of a high energy facet as a means of controlling the shapes of TiO_2 nanocrystals, J. Am. Chem. Soc. 125 (2003) 15981–15985.

[23] H. G. Yang, Anatase TiO_2 single crystals with a large percentage of reactive facets. Nature 453 (2008) 638–641.

[24] V. Berbenni, A. Marini, G. Bruni, Effect of mechanical activation on the preparation of $SrTiO_3$ and Sr_2TiO_3 ceramics from the solid state system $SrCO_3$ –TiO_2, J. Allo. Compd. 329 (2001) 230–238

[25] M.K. Rath, G.K. Pradhan, B. Pandey, H.C. Verma, B.K. Roul, S. Anand, Synthesis, characterization and dielectric properties of europium-doped barium titanate nanopowders, Mater. Lett. 62 (2008) 2136–2139.

[26] S. Ohara, A. Kondo, H. Shimoda, K. Sato, H. Abe, M. Naito, Rapid mechanochemical synthesis of fine barium titanate nanoparticles, Mater. Lett. 62 (2008) 2957–2959.

[27] R. Ashiri, Detailed FTIR spectroscopy characterization and thermal analysis of synthesis of barium titanate nanoscale particles through a newly developed process, Vib. Spectrosc. 66 (2013) 24–29.

[28] K.-H. Felgner, T. Muller, H.T. Langhammer, H.-P. Abicht, On the formation of $BaTiO_3$ from $BaCO_3$ and TiO_2 by microwave and conventional heating, Mater. Lett. 58 (2004) 1943–1947.

[29] P. Ren, H. Fan, X. Wang, K. Liu, A novel approach to prepare tetragonal $BaTiO_3$ nanopowders, Mater. Lett. 65 (2011) 212–214.

[30] T.V. Anuradha, S. Ranganathan, T. Mimani, K.C. Patil, Combustion synthesis of nanostructured barium titanate, Scripta Mater. 44 (2001) 2237–2241.

[31] J. Zeng, Ch. Lin, J. Li, Kun Li, Low temperature preparation of barium titanate thin films by a novel sol–gel–hydrothermal method, Mater. Lett. 38 (1999) 112–115.

[32] Ch.-Y. Fang, Ch. Wang, A.V. Polotai, D. K. Agrawal, M.T. Lanagan, Microwave synthesis of nano-sized barium titanate, Mater. Lett. 62 (2008) 2551–2553.

[33] T. Sahoo, S.K. Tripathy, M. Mohapatra, S. Anand, R.P. Das, X-ray diffraction and microstructural studies on hydrothermally synthesized cubic barium titanate from TiO_2–$Ba(OH)_2$–H_2O system, Mater. Lett. 61 (2007) 1323–1327.

[34] D.F.K. Hennings, B.S. Schreinemacher, H. Schreinemacher, Solid-State preparation of $BaTiO_3$-based dielectrics, using ultrafine raw materials, J. Am. Ceram. Soc. 84 (2001) 2777–82.

[35] R. Ashiri, A. Nemati, M. Sasani Ghamsari, S. Sanjabi, M. Aalipour, A modified method for barium titanate nanoparticles synthesis, Mater. Res. Bull. 46 (2011) 2291–2295.

[36] A. Heidary Moghadam, V. Dashtizad, A. Kaflou, H. Yoozbashizadeh, R. Ashiri, Development of a nanostructured Zr3Co intermetallic getter powder with enhanced pumping characteristics, Intermetallics 57 (2015) 51–59.

[37] P.Balaz, B.Plesingerova, Thermal Properties of Mechanochemically Pretreated Precursors of $BaTiO_3$ Synthesis, J. Therm. Anal. Calor. 59 (2000) 1017-1021.

[38] P.Balaz, J. Briancin, Z. Bastl, L. Medvecky, V. Sepelak, Properties of mechanochemically pretreated precursors of doped $BaTiO_3$ ceramics, J. Mat. Sci. 29 (1994) 4847-4851.

[39] R.Yanagawa, M. Senna, C. Ando, H. Chazono, H. Kishi, Preparation of 200 nm $BaTiO_3$ particles with their tetragonality 1.010 via a solid-state reaction preceded by agglomeration-free mechanical activation, J. Am. Chem. Soc. 90 (2007) 809-814.

[40] R. Ashiri, A. Nemati and M. Sasani Ghamsari, H. Adelkhani, Characterization of optical properties of amorphous BaTiO3 nanothin films. J. Non-Cryst. Sol. 355 (2009) 2480-2484.

[41] R. Ashiri□, A. Moghtada, A. Shahrouzianfar, Processing and characterization of carbonate-free BaTiO3 nanoscale particles obtained by a rapid ultrasound-assisted wet chemical approach, Metall. Mat. Trans. B46, Metall. Mat. Trans. B46 (2015) 1912-1923.

[42] R. Ashiri, A. Moghtada, Carbonate-free strontium titanium oxide nanosized crystals with tailored morphology: facile synthesis, characterization, and formation mechanism, Metall. Mater. Trans. B45 (2014) 1979-1986.

[43] R. Ashiri, A mechanistic study of nanoscale structure development, phase transition, morphology evolution, and growth of ultrathin barium titanate nanostructured films, Metall. Mat. Trans. A45 (2014) 4138-4154.

[44] R. Ashiri, R. Ajami, A. Moghtada, Sonochemical synthesis of SrTiO3 nanocrystals at low temperature, Int. J. Appl. Ceram. Technol. 12 (2015) E202-E206.

[45] R. Ashiri, A. Moghtada, A. Shahrouzianfar, R. Ajami, Low temperature synthesis of carbonate-free barium titanate nanoscale crystals: toward a generalized strategy of titanate-based perovskite nanocrystals synthesis, J. Am. Ceram. Soc. 97 (2014) 2027-2031.

[46] R. Ashiri, A. Nemati, M. Sasani Ghamsari, Crack-free nanostructured BaTiO3 thin films prepared by sol–gel dip-coating technique, Ceram. Int. 40 (2014) 8613-8619.

[47] R. Ashiri, Analysis and characterization of relationships between the processing and optical responses of amorphous BaTiO3 nanothin films obtained by an improved wet chemical process, Metall. Mater. Trans. B45 (2014) 1472-1483.

[48] F. Davar, M.R. Loghman-Estarki, R. Ashiri, From inorganic/organic nanocomposite based on chemically hybridized CdS–TGA to pure CdS nanoparticles, J. Ind. Eng. Chem. 21(2015) 965- 970.

[49] F. Davar, M.R. Loghman-Estarki, M. Salavati-Niasari, R. Ashiri: Synthesis of volcano-like CdS/organic nanocomposite, Int. J. Appl. Ceram. Technol. 11(2014) 637-644.

[50] R. Ashiri, A. Nemati, M. Sasani Ghamsari, M. M. Dastgahi, Nanothickness films, nanostructured films, and nanocrystals of barium titanate obtained directly by a newly developed sol–gel synthesis pathway, J. Mater. Sci. Mater. Electron. 25 (2014) 5345-5355.

[51] R. Ashiri, A new sol–gel processing routine without chelating agents for preparing highly transparent solutions and nanothin films: engineering the role of chemistry to design the process, Phil. Mag. 95 (2015) 1-11.

[52] R. Ashiri, Development and investigation of novel nanoparticle embedded solutions with enhanced optical transparency, J. Mater. Res. 29 (2014) 2949-2956.

[53] H. Kalhori, A. Irajizad, A. Azarian, R. Ashiri, Synthesis and characterization of electrochemically grown CdSe nanowires with enhanced photoconductivity, J. Mater. Sci. Mater. Electron. 26 (2015) 1395–1402.

[54] A. Moghtada, R. Ashiri, Nanocrystals of $XTiO_3$ (X=Ba, Sr, Ni, BaxTi1-x) materials obtained through a rapid one-step methodology at 50 °C, Ultrason. Sonochem. 26 (2015) 293–304.

[55] A. Modabberasl, P. Kameli, M. Ranjbar, H. Salamati, R. Ashiri, Fabrication of DLC thin films with improved diamond-like carbon character by the application of external magnetic field, Carbon 94 (2015) 485–493.

[56] A. Moghtada, A. Shahrouzianfar, R. Ashiri, Facile synthesis of $NiTiO_3$ yellow nano-pigments with enhanced solar radiation reflection efficiency by an innovative one-step method at low temperature, Dyes .Pigments. 123 (2015) 92-99.

[57] R. Ashiri, A. Heidary Moghadam, R. Ajami, Obtaining the highly pure barium titanate nanocrystals by a new approach, J. Alloy. Compd. 648 (2015) 265-268.

[58] R. Ashiri, Obtaining a novel crystalline/amorphous core/shell structure in barium titanate nanocrystals by an innovative one-step approach, RSC Adv. 5 (2015) 48281-48289.

Figure captions

Fig. 1. Flowchart showing the stepwise method of preparation of carbonate-free BTO nanocrystals used in this work.

Fig. 2. SEM micrographs of the TiO_2 and $BaCO_3$ starting materials showing their particles size and morphology.

Fig. 3. XRD patterns of (a) TiO_2 and (b) $BaCO_3$ starting powders as received and after different milling (mechanical activation) times.

Fig. 4. Effect of mechanical activation time on particle size and morphology of the starting materials.

Fig. 5. Polyhedra structures for the TiO_2 polymorphs: (a) anatase and (b) rutile. Ti and O atoms are represented by big blue and small red spheres, respectively.

Fig. 6. XRD patterns of TiO_2 and $BaCO_3$ starting and activated powders, and after their mixing for 4 h.

Fig. 7. SEM micrographs showing the mixture of the powders after 4 h milling: (a) mixture of TiO_2 and $BaCO_3$ starting powders, (b) mixture of TiO_2 and $BaCO_3$ powders activated for 10 h and (c) mixture of TiO_2 and $BaCO_3$ powders activated for 30 h.

Fig. 8. DTA curves of the mixture of (a) as- received starting materials and (b) mechanically activated (10 h) BCO and TiO_2 powders showing the effect of mechanical activation of the starting materials on the kinetic of formation of BTO.

Fig. 9. XRD patterns of BTO nanocrystals synthesized under different preparation conditions.

Fig. 10. FE-SEM micrographs at different magnifications of BTO nanocrystals synthesized under different preparation conditions.

Fig. 11. EDAX results of BTO nanocrystals synthesized in this work (a) with and (b) without mechanical activation of the starting materials.

Figure 1

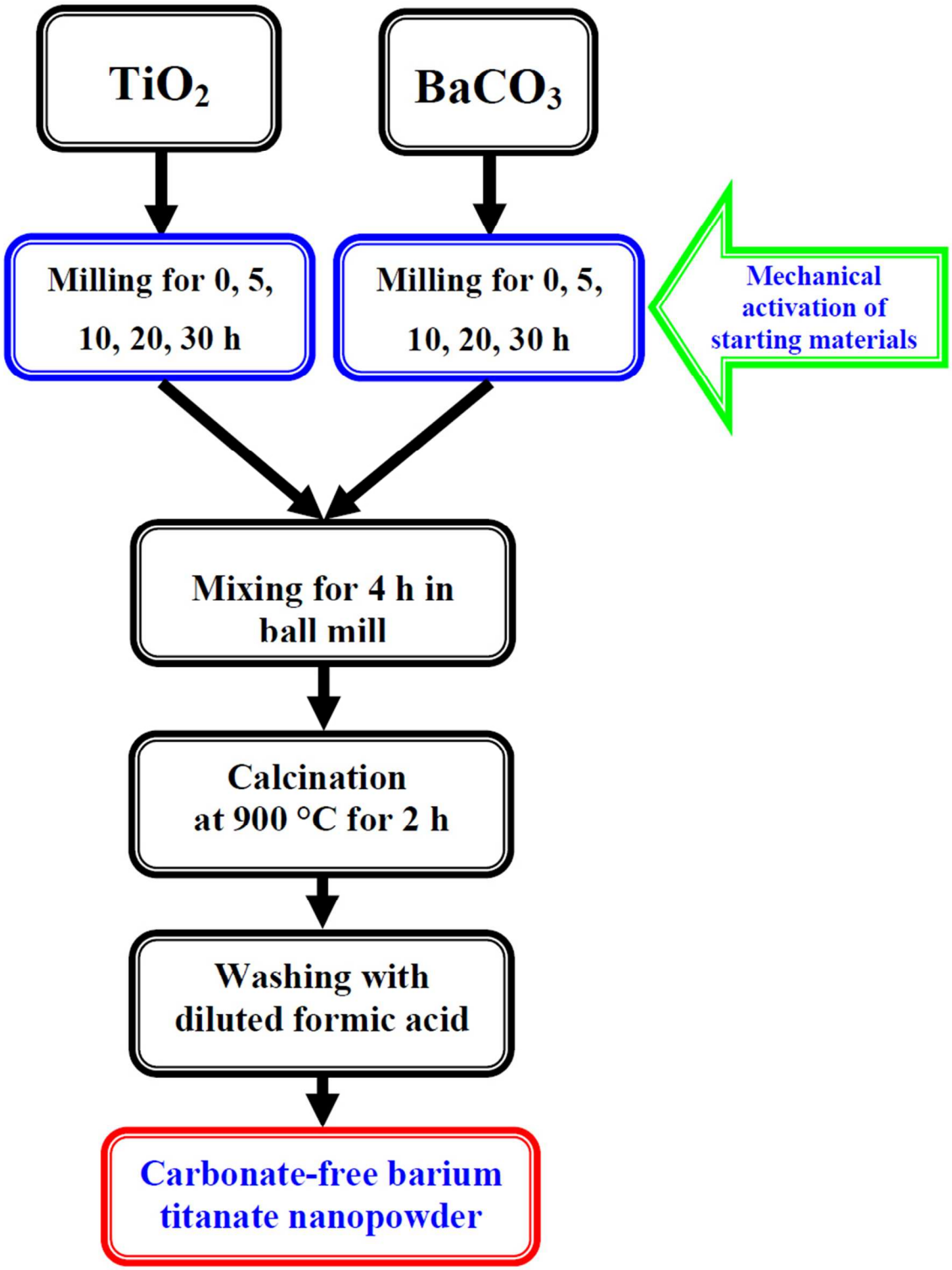

Fig. 1. Flowchart showing the stepwise method of preparation of carbonate-free BTO nanocrystals used in this work.

Figure 2

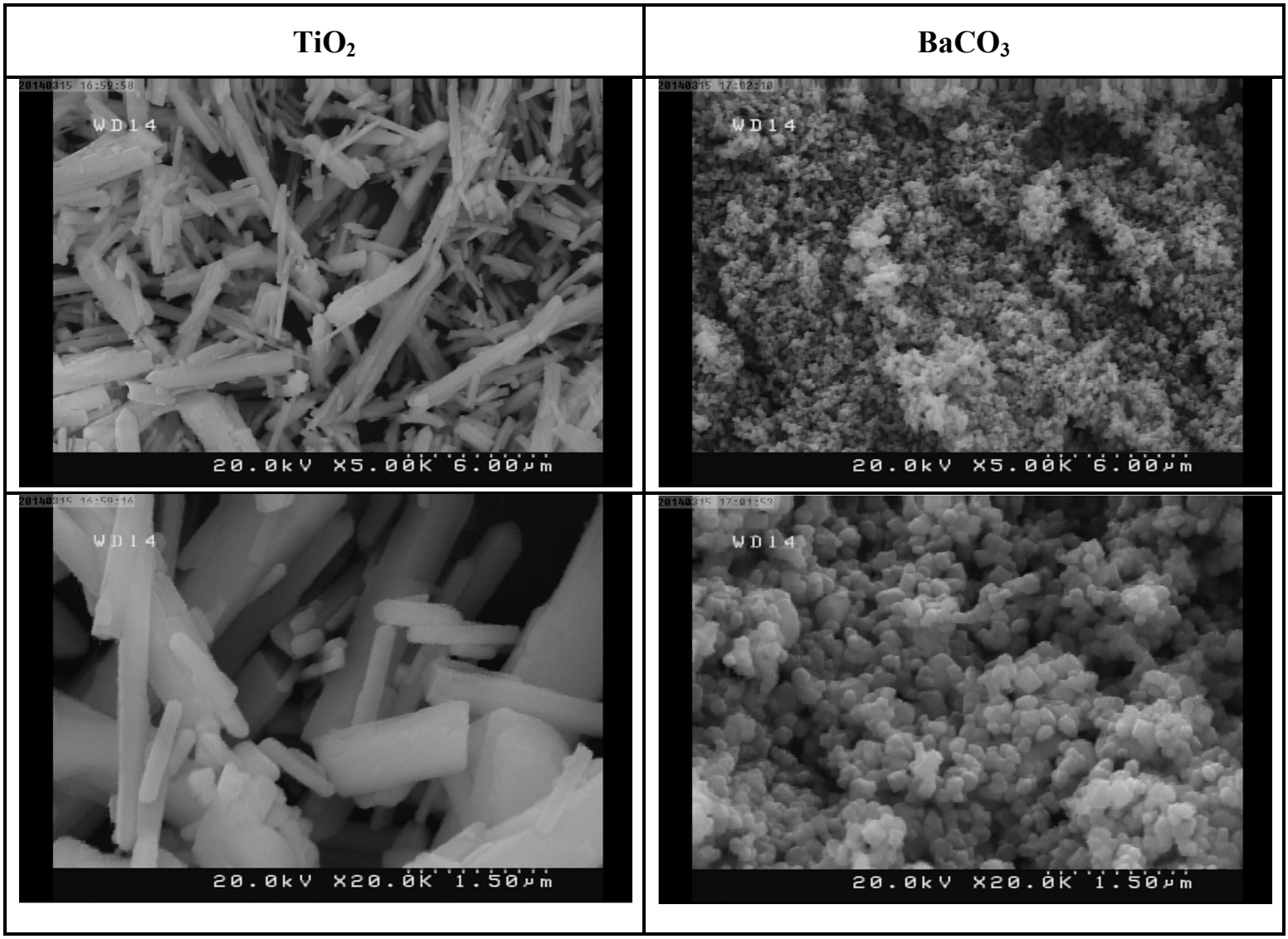

Fig. 2. SEM micrographs of the TiO_2 and $BaCO_3$ starting materials showing their particles size and morphology.

Figure 3a

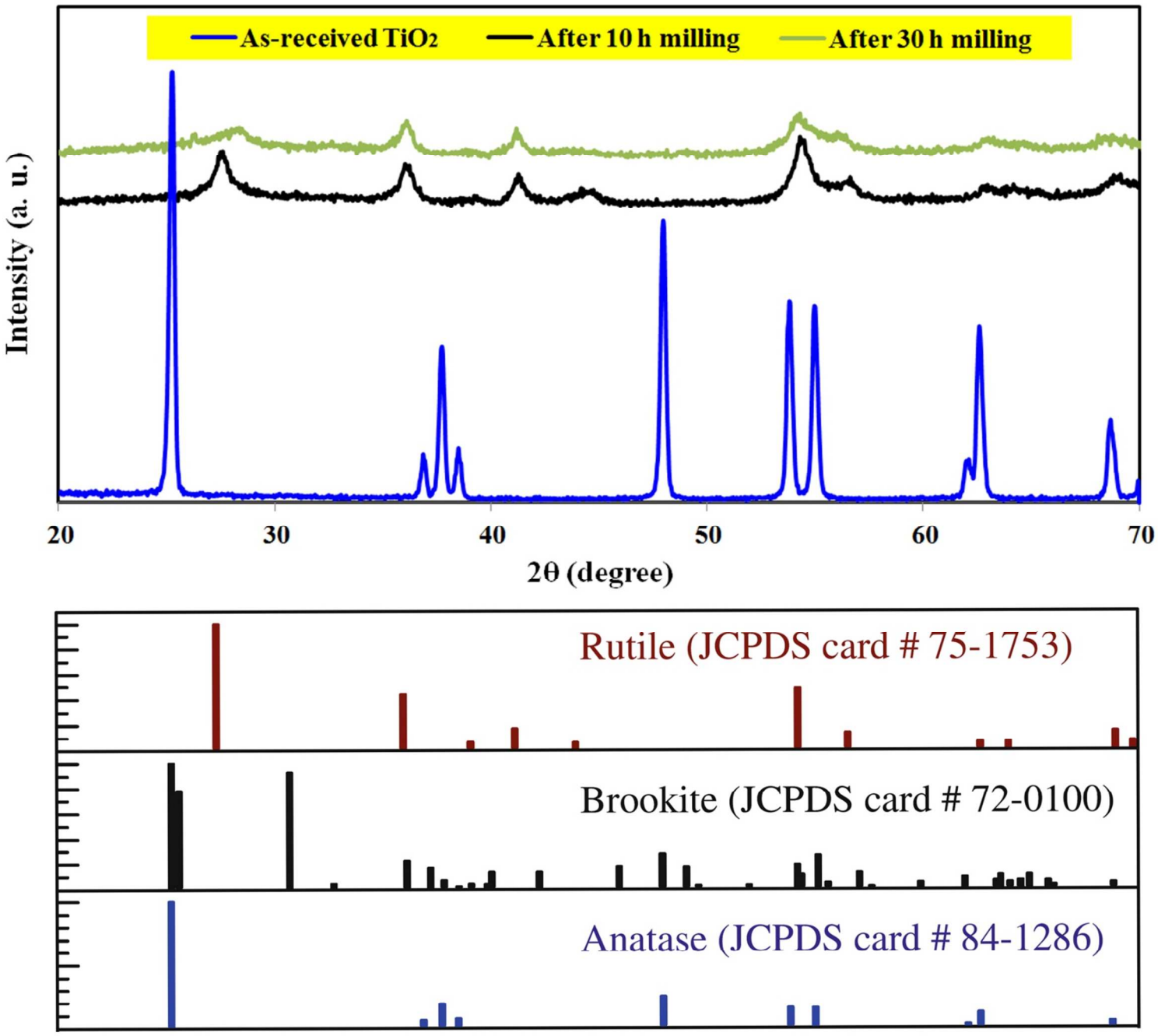
As-received TiO2
After 10 h milling
After 30 h milling
Intensity (a. u.)
20
30
40
50
60
70
2θ (degree)
Rutile (JCPDS card # 75-1753)
Brookite (JCPDS card # 72-0100)
Anatase (JCPDS card # 84-1286)

Figure 3b

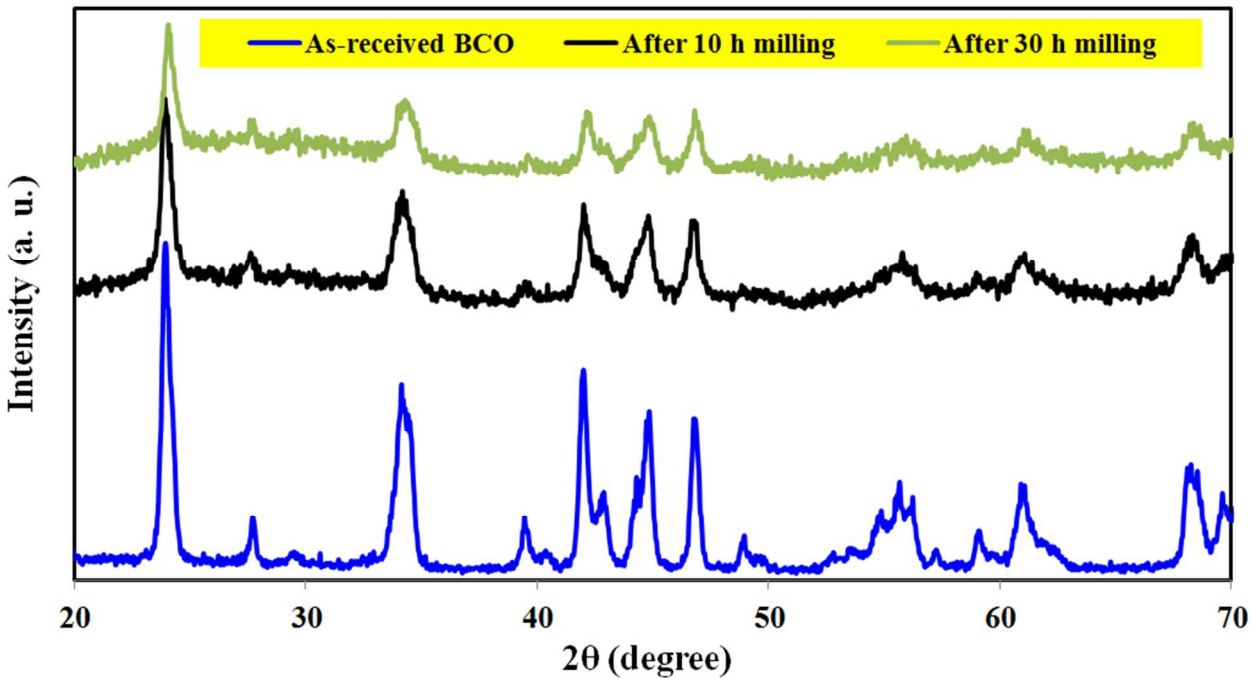

Fig. 3. XRD patterns of (a) TiO_2 and (b) $BaCO_3$ starting powders as received and after different milling (mechanical activation) times.

Figure 4

Mechanical activation time	TiO_2	$BaCO_3$
0 h	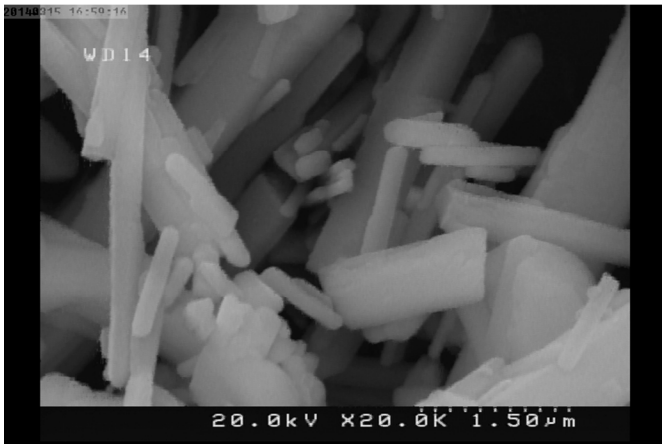	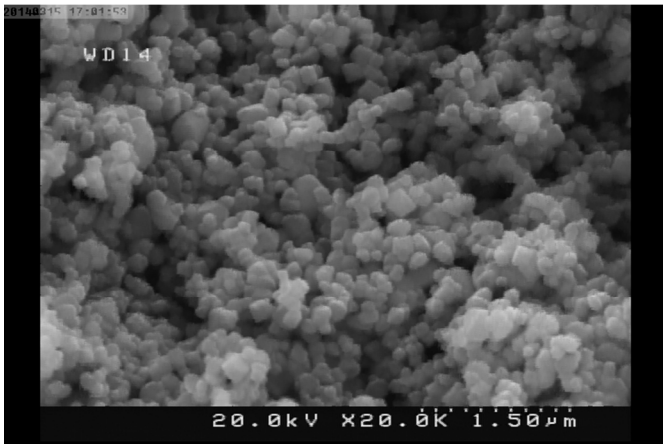
10 h	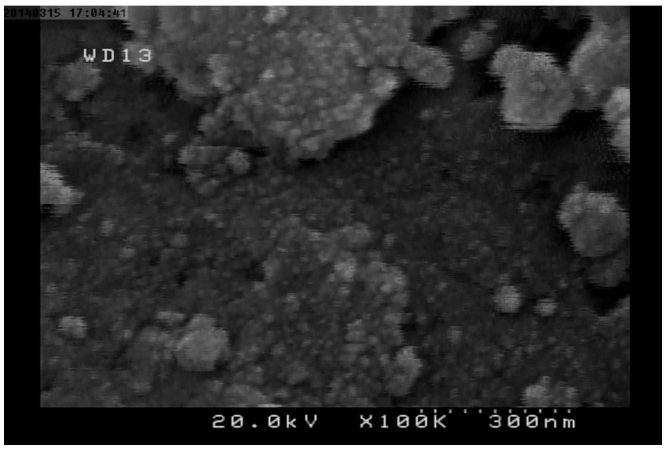	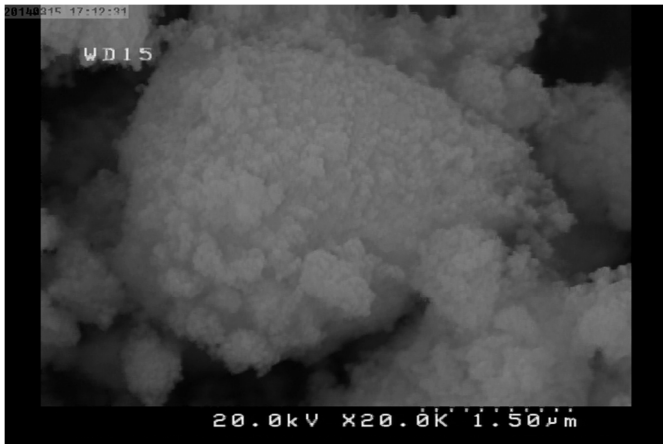
30 h	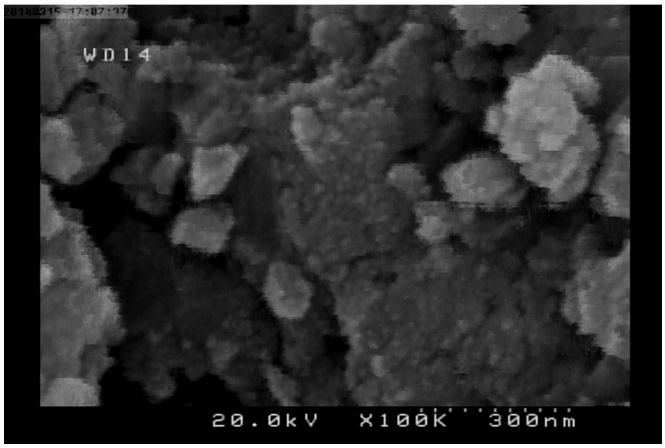	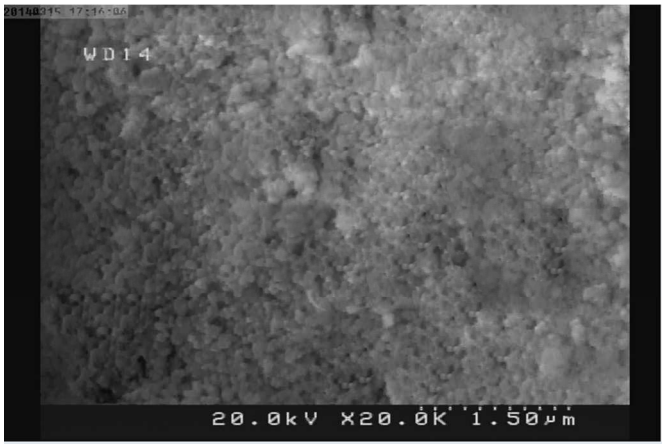

Fig. 4. Effect of mechanical activation time on particle size and morphology of the starting materials.

Figure 5

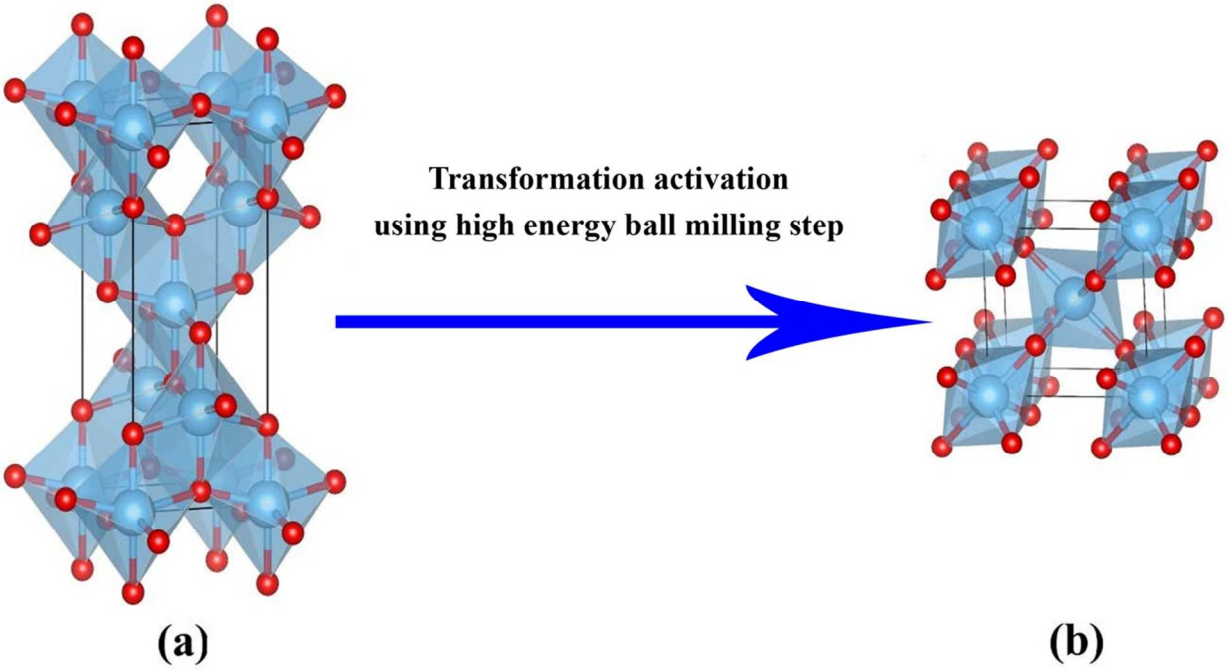

Fig. 5. Polyhedra structures for the TiO_2 polymorphs: (a) anatase and (b) rutile. Ti and O atoms are represented by big blue and small red spheres, respectively.

Figure 6

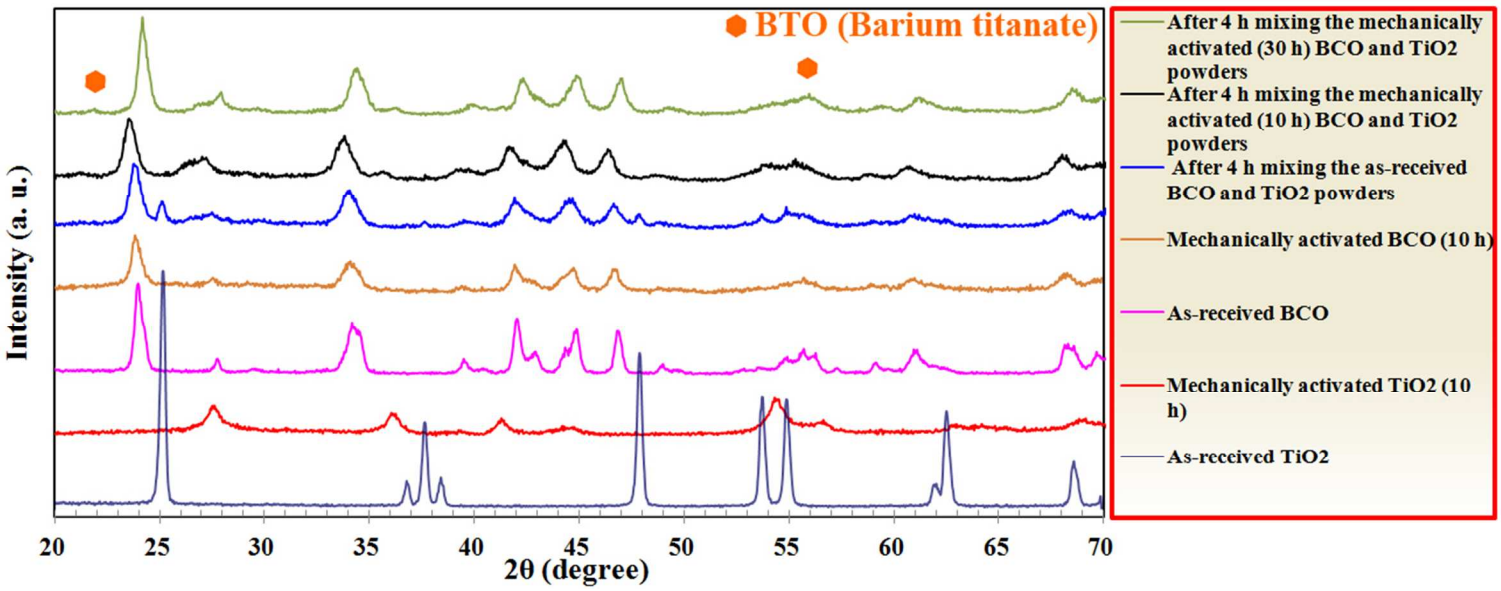

Fig. 6. XRD patterns of TiO_2 and $BaCO_3$ starting and activated powders, and after their mixing for 4 h.

Figure 7

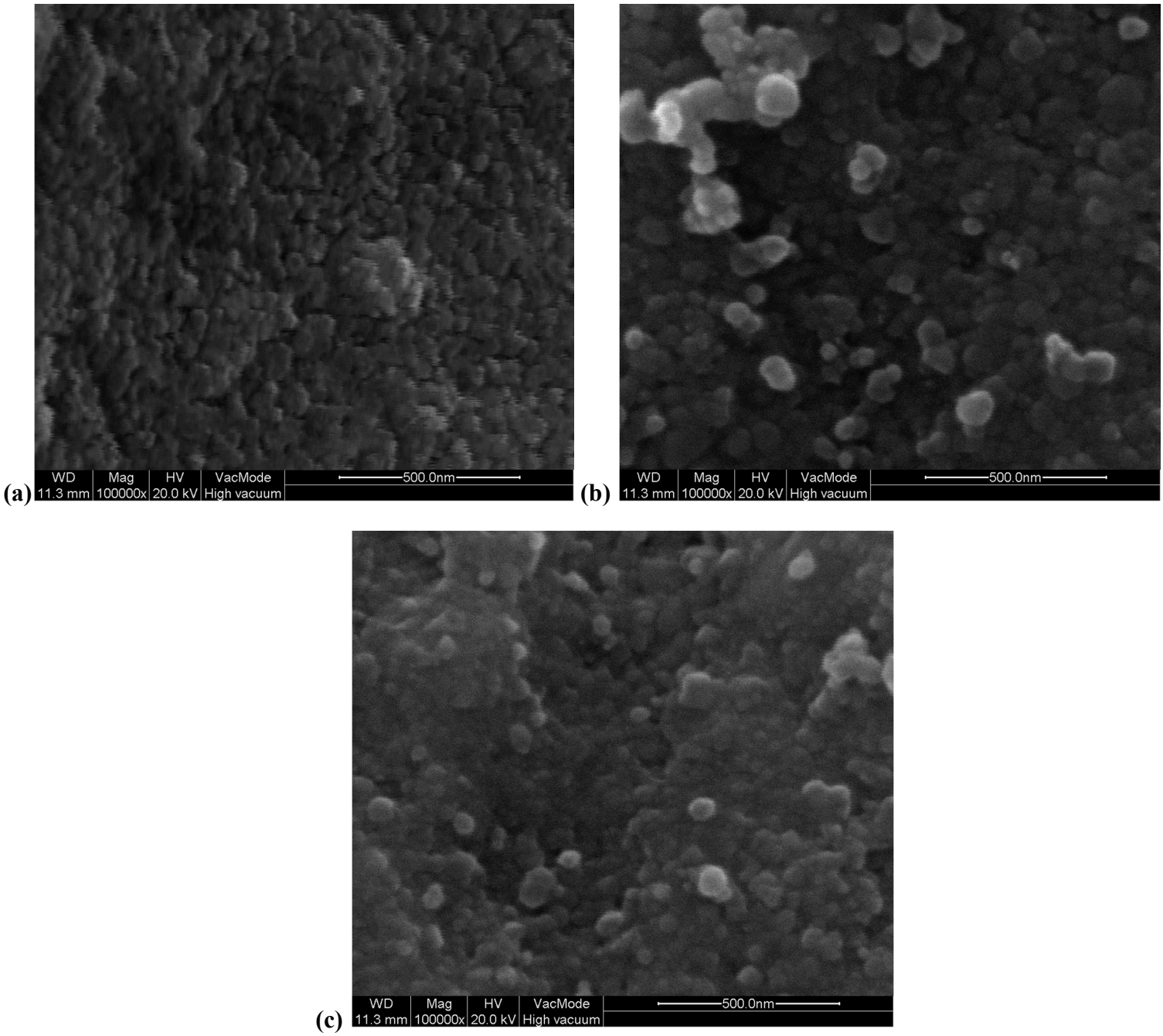

Fig. 7. SEM micrographs showing the mixture of the powders after 4 h milling: (a) mixture of TiO_2 and $BaCO_3$ starting powders, (b) mixture of TiO_2 and $BaCO_3$ powders activated for 10 h and (c) mixture of TiO_2 and $BaCO_3$ powders activated for 30 h.

Figure 8

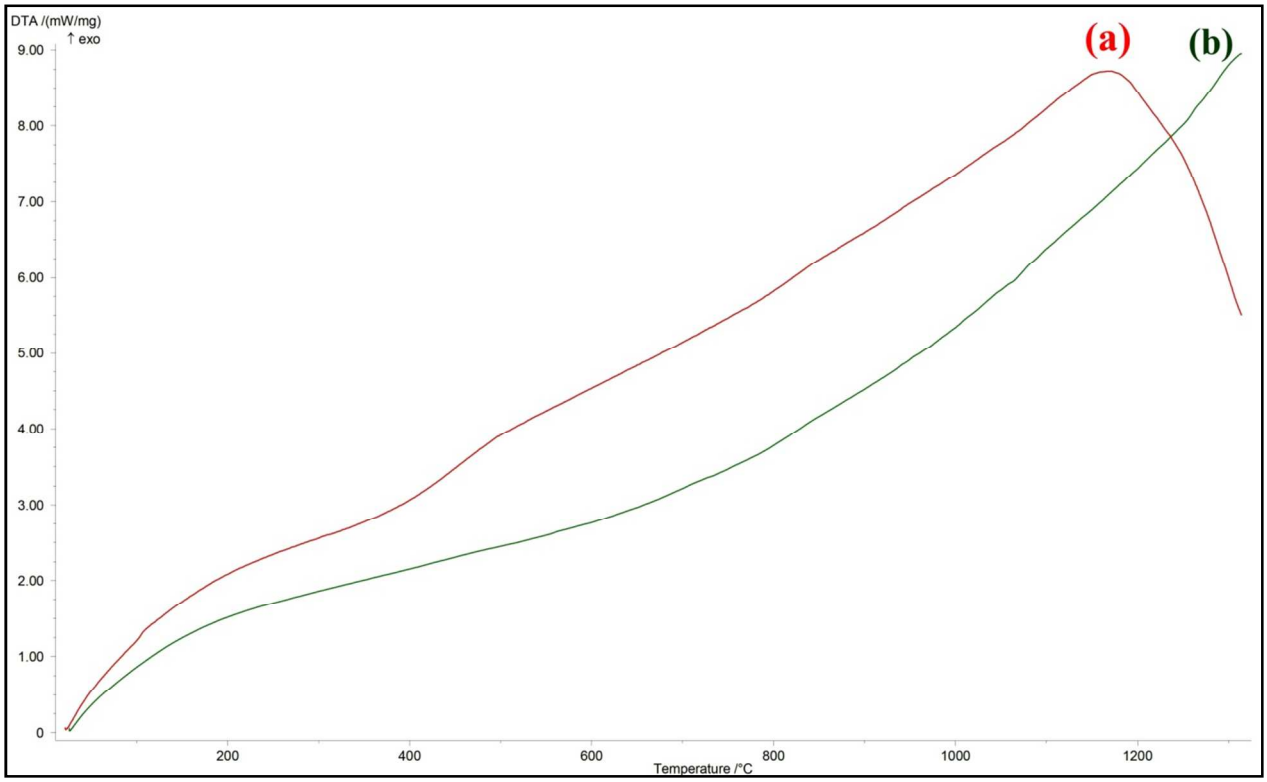

Fig. 8. DTA curves of the mixture of (a) as- received starting materials and (b) mechanically activated (10 h) BCO and TiO_2 powders showing the effect of mechanical activation of the starting materials on the kinetic of formation of BTO.

Figure 9

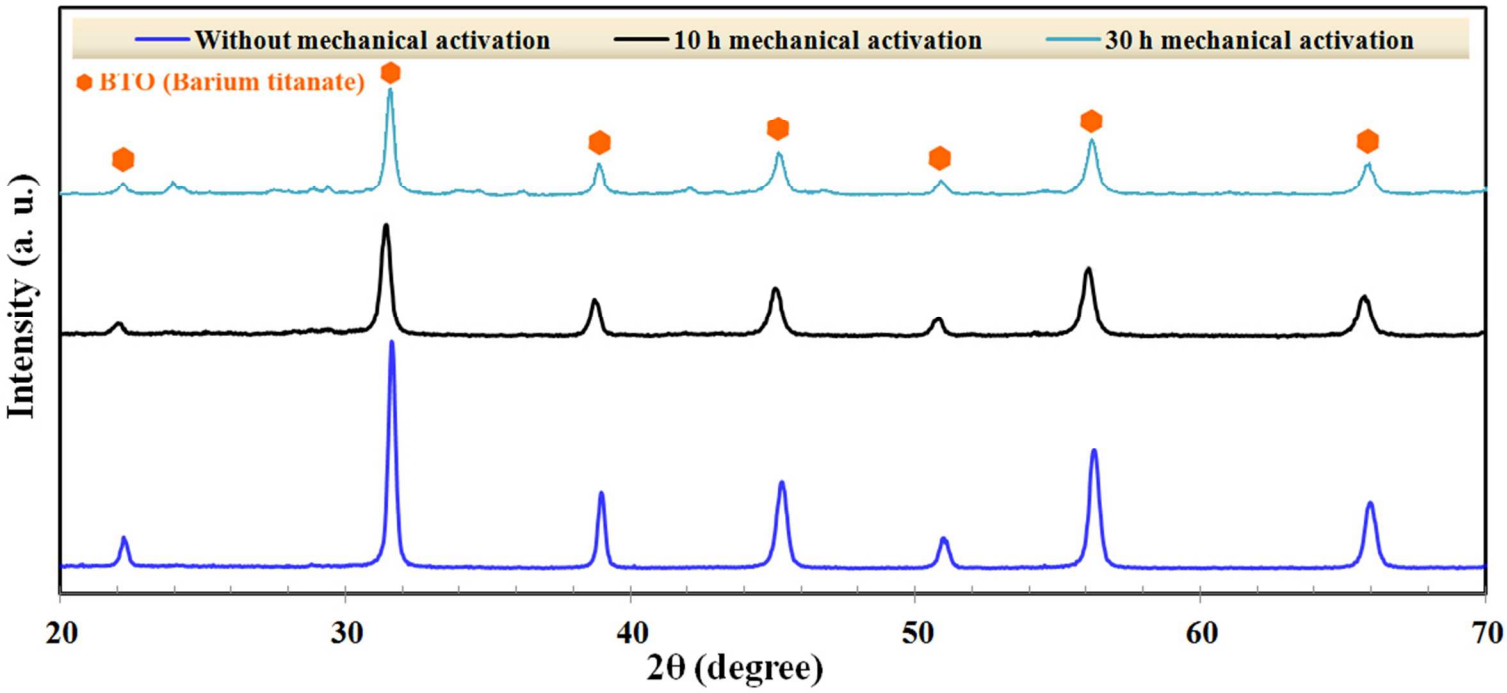

Fig. 9. XRD patterns of BTO nanocrystals synthesized under different preparation conditions.

Figure 10

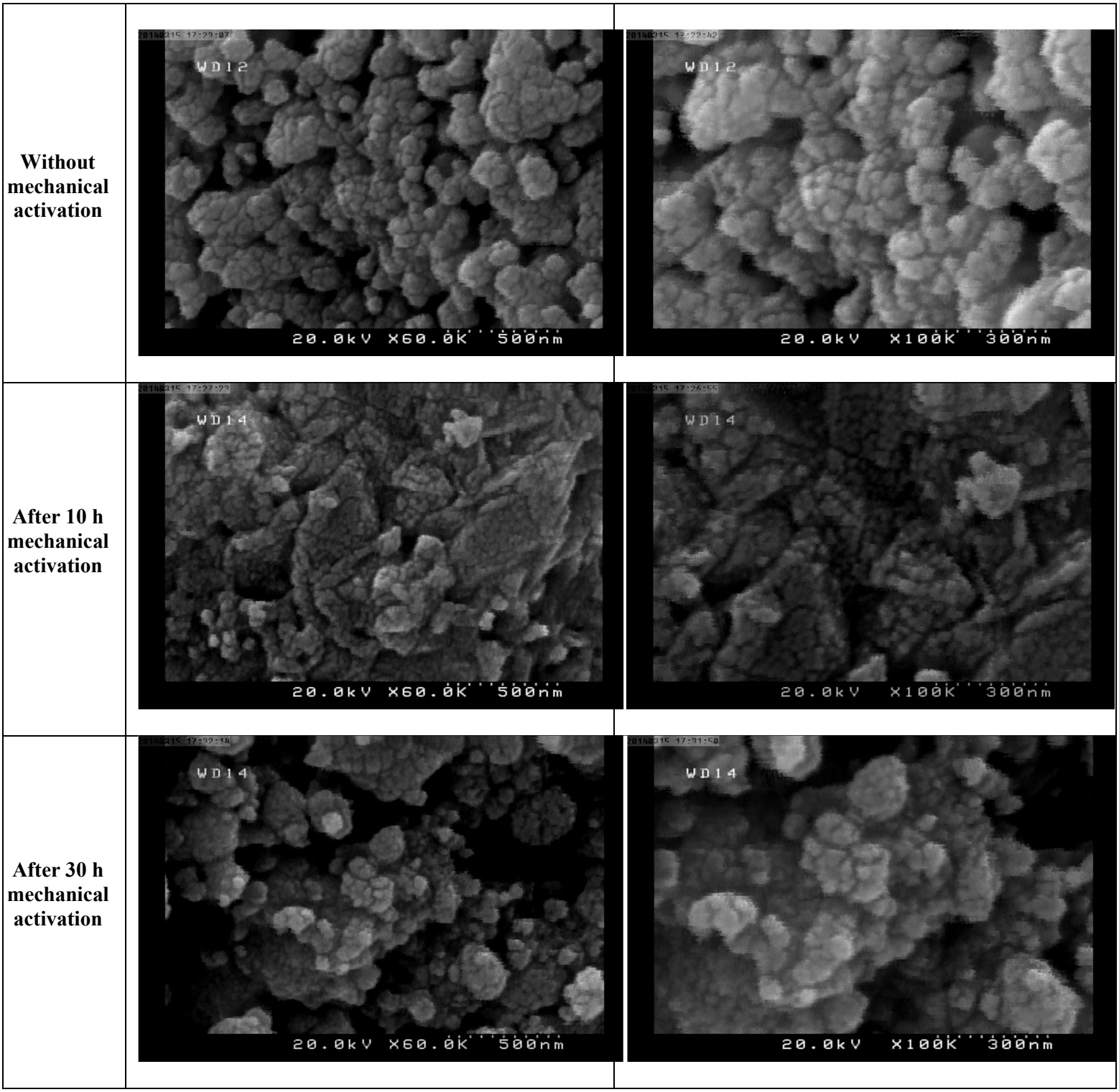

Fig. 10. FE-SEM micrographs at different magnifications of BTO nanocrystals synthesized under different preparation conditions.

Figure 11

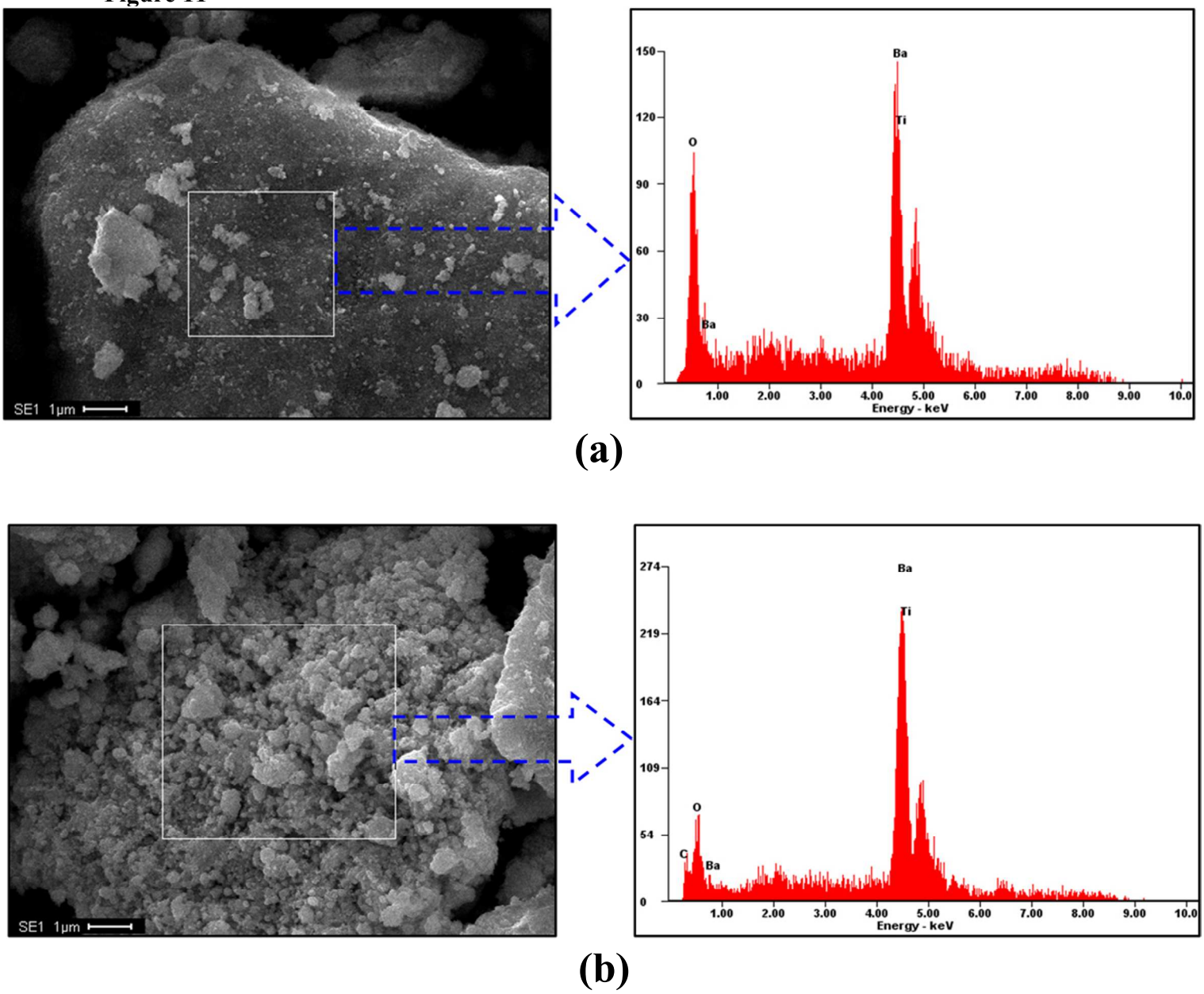

Fig. 11. EDAX results of BTO nanocrystals synthesized in this work (a) with and (b) without mechanical activation of the starting materials.